ISSN 0021-3640, JETP Letters, 2024, Vol. 119, No. 6, pp. 444–450. © The Author(s), 2024. This article is an open access publication.
Russian Text © The Author(s), 2024, published in Pis'ma v Zhurnal Eksperimental'noi i Teoreticheskoi Fiziki, 2024, Vol. 119, No. 6, pp. 432–438.

CONDENSED MATTER

# Features of a Low-Temperature Charge Density Wave in the Monoclinic Phase of $NbS_3$ Manifested in the NMR and in Transport Properties

**A. S. Semakin[a], I. R. Mukhamedshin[b], S. G. Zybtsev[c], and V. Ya. Pokrovskii[c,*]**

[a] *Wihuri Physical Laboratory, Department of Physics and Astronomy, University of Turku, 20014 Turku, Finland*
[b] *Université Paris-Saclay, CNRS, Laboratoire de Physique des Solides, 91405 Orsay, France*
[c] *Kotelnikov Institute of Radioengineering and Electronics, Russian Academy of Sciences, Moscow, 125009 Russia*
**e-mail: vadim.pokrovskiy@mail.ru*

Received February 9, 2024; revised February 9, 2024; accepted February 15, 2024

The relaxation of the transverse nuclear magnetization in the monoclinic phase of $NbS_3$ has been studied by the $^{93}$Nb nuclear magnetic resonance method near the temperature $T_{P2} = 150$ K, at which a low-temperature charge density wave is formed. It has been shown that the critical slowing down of one of the vibrational modes of the lattice, which is quite slow even above $T_{P2}$, occurs slightly below $T_{P2}$. The transition at $T_{P2}$ occurs not only in low-resistance samples, as thought previously, but also in high-resistance ones, and involves Nb atoms in the bulk of a sample. The transport properties of high-resistance samples, namely, the smearing of the depinning threshold for the charge density wave below $T_{P2}$, confirm that the phase transition in them occurs at $T_{P2}$. It has been concluded that the distortion of the lattice at $T_{P2}$ is not due to the Peierls mechanism and can be attributed to the Keldysh–Kopaev transition. Another possible mechanism is the fluctuation distortion of the lattice above $T_{P2}$ that prevents the sliding of the charge density wave.

**DOI:** 10.1134/S0021364024600435

The monoclinic phase of $NbS_3$ ($NbS_3$-II) is remarkable due to the existence of two charge density waves CDW-0 and CDW-1 at room temperature and of the third charge density wave CDW-2 formed at 150 K (see [1] and references therein). The diversity of charge density waves in $NbS_3$-II is obviously caused by a complex structure of the unit cell. Eight chains of Nb atoms surrounded by trigonal prisms of S atoms intersect the unit cell of this polytype in the (010) section parallel to the **a** and **c** axes. According to the structural data reported in [2], the area of the unit cell $s_0$ in the (010) section is 180 Å$^2$. The formation temperatures of the charge density waves CDW-0 and CDW-1 are found to be $T_{P0} \approx 470$ K and $T_{P1} \approx 360$ K, respectively, and the corresponding wave vectors are $\mathbf{q}_0 = (0, 0.352, 0)$ and $\mathbf{q}_1 = (0, 0.298, 0)$ [2–4].

The charge density wave CDW-2 is formed at $T_{P2} = 150$ K and is manifested in the transport properties of only low-resistance samples with the conductivity $\sigma_s(300\text{ K})$ in the range of 10–300 $(\Omega\text{ cm})^{-1}$ [1]. The formation of the "low-temperature" CDW-2 is manifested in a step of the conductivity $\delta\sigma_{s2}$ near $T_{P2}$. The nonlinear conductivity caused by the sliding of CDW-2 is observed below $T_{P2}$. In this respect, the transition at $T_{P2}$ is similar to the transitions observed at $T_{P1}$ and $T_{P0}$, but distortions of the lattice below $T_{P2}$ have not yet been observed.

A feature near $T_{P2}$ was also observed in the studied of thermal electromotive force [5]. High-resistance samples below $T_{P1}$ exhibit properties of intrinsic semiconductors, whereas low-resistance samples are similar to doped semiconductors, where electrons coming from impurities (defects and vacancies) to the conduction band are condensed in CDW-2 [5]. Correspondingly, the charge density carried by CDW-2 depends on the sample. The number of chains in the unit cell contributing to the current of the charge density wave can be determined in terms of the ratio of the current density $j_{CDW}$ of the charge density wave to the fundamental frequency $f$ of sliding of the charge density wave [1] as $N_{ch} \equiv s_0 j_{CDW}/(2ef)$. The numbers $N_{ch}$ for CDW-1 and CDW-0 are about 1 [1, 3], which seems reasonable. The number $N_{ch}$ for CDW-2 is in the range of $10^{-3}$–1/3 [1], i.e., less than one chain per unit cell in any case. Comparing the samples with different conductivities, we concluded that $N_{ch}$ is proportional to the jump $\delta\sigma_{s2}$ [1]. A deficit of sulfur was also observed in low-resistance samples [1].

The photoconductivity of CDW-2 is also anomalous. In contrast to charge density waves in some other

materials and to CDW-1 in $NbS_3$-II, the action of near infrared radiation results in a decrease rather than an increase in the depinning threshold field $E_t$ of this charge density wave [6].

$NbS_3$ whiskers feature numerous stacking faults. Stacking faults in phase I were reported in [7]. Stacking faults in phase II were observed in a scanning tunneling microscope and in a transmitting electron microscope [4, 8, 9] in the form of atomic rows parallel to the **b** axis in the (100) plane. These rows usually differ in an extra period in the **c** direction [9]. It was concluded that stacking faults are planes parallel to the (001) plane, i.e., perpendicular to the **c** axis along which the bond is the weakest [8]. The structural modulation with a period of about 2.1 **b** is sometimes observed in the region of stacking faults on scanning tunneling microscopy images obtained below 150 K [9]. It was presumably associated with CDW-2, but it appeared impossible to monitor a change in the structure of the same region of stacking faults at decreasing temperature below $T_{P2}$.

The resulting hypothetical picture is as follows: CDW-2 is formed on stacking faults, were sulfur vacancies are likely concentrated [4, 9]. The larger the number of vacancies, the higher the concentration of stacking faults, correspondingly, the charge density of CDW-2 [1]. Thus, CDW-2 consists of atomically thin planes located in the bulk of the crystal; i.e., it is a set of two-dimensional layers. This picture seems more realistic after the observation of charge density waves on dichalcogenide monolayers [10–12].

Transitions at $T_{P1}$ and $T_{P2}$ were also observed in NMR experiments [1]. $^{93}$Nb NMR spectra were measured in an unoriented "batting" consisting of high- and low-resistance whiskers. The transition at $T_{P1}$ is clearly identified by a change in the Knight shift of the central NMR line by 0.05% near 360 K, which indicates a change in the carrier density on chains. No shift of NMR lines was observed near $T_{P2}$, but the maximum relaxation rate of the transverse nuclear magnetization $T_2^{-1}$ was observed near 130 K slightly below the transition. The feature was attributed to the freezing of one of the phonon modes, which leads to the periodic distortion of the electron density at cooling. This conclusion is confirmed by the fact that a similar maximum was observed in $NbSe_3$ also slightly below the formation temperature of one of the charge density waves (CDW-1) [13]. At the same time, unlike $NbS_3$-II [1], the maximum relaxation rate $T_1^{-1}$ of the *longitudinal* nuclear magnetization was in addition observed in $NbSe_3$ at the same temperature.

Since the sample studied in [1] was a mixture of high- and low-resistance whiskers, we could not determine in which of them the phonon mode was frozen. Furthermore, the NMR measurements in unoriented samples did not indicate which of the nonequivalent chains in $NbS_3$-II were involved thein transition at $T_{P2}$.

In this work, we perform the NMR study of samples composed of whiskers oriented along the **b** axis. We prepared one predominantly high-resistance sample and one predominantly low-resistance sample. The transition near $T_{P2}$ in both samples is clearly identified by the maximum in the temperature dependence $T_2^{-1}(T)$ of the relaxation rate of the transverse nuclear magnetization of $^{93}$Nb. This transition involves Nb atoms in all unit cells of $NbS_3$-II rather than only on stacking faults. The result is explained under the assumption that CDW-2 also exists above 150 K but moves in the state coupled with one-dimensional fluctuations. It is also confirmed by experimental data on the transport properties of the high-resistance samples $NbS_3$-II.

Developing the method used in [1], we prepared sets of oriented whiskers $NbS_3$-II from two different grown series with the prevalence of low-resistance (sample P2a) and high-resistance crystals (sample P2b) for measurements. The selected whiskers were carefully placed on an adhesive tape in parallel to each other (see the inset of Fig. 1c). Then, this tape was cut into 3-mm-wide strips, which were stacked, so that the **b** axes of whiskers were parallel. This allowed measurements in the magnetic field **H** oriented both along the crystallographic **b** axis of the whiskers ($\mathbf{H} \parallel \mathbf{b}$) and across it ($\mathbf{H} \perp \mathbf{b}$). The mass of whiskers in the resulting samples was slightly below 30 mg. We used a superconducting solenoid providing a static magnetic field of $B = 7.5535$ T with a uniformity better than 10 ppm in the studied 20 × 3 × 3-mm samples. A standard two-pulse sequence of rf pulses was used to measure spin-echo signals in the region of the central $^{93}$Nb NMR line with a frequency step of 100 kHz, and the NMR spectrum was then reconstructed by a Fourier transform [14].

Figure 1a presents spectra of the central $^{93}$Nb NMR line corresponding to the $-1/2 \rightarrow +1/2$ transition for the sample P2a at a temperature of 100 K. Low-resistance whiskers prevail in this sample. The measurements were carried out at different repetition times of the pulse sequence. Three nonequivalent groups of lines marked by the letters A, B, and C in Fig. 1a can be identified in the spectra. The intensity of the line A hardly depends on the repetition time, whereas the intensity of the line B decreases slightly with reducing repetition time. Nevertheless, the spin relaxation times on $^{93}$Nb nuclei corresponding to both lines can be considered as small compared to the group of lines C, which is almost completely suppressed with decreasing repetition time (see Fig. 1a).

The nuclear relaxation is caused by fluctuating fields on $^{93}$Nb nuclei, which are induced in the $NbS_3$ compound by charge carriers. Therefore, NMR sig-

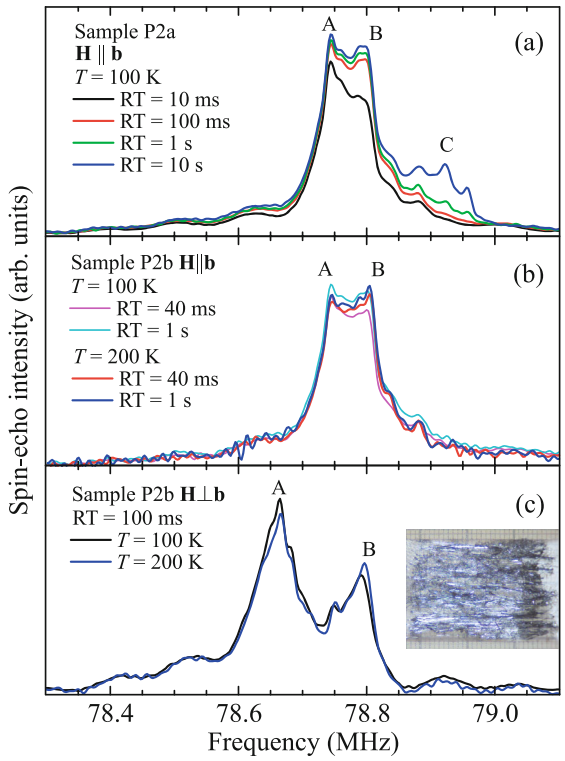


**Fig. 1.** (Color online) Spectra of the central $^{93}$Nb NMR line in the samples P2a (low-resistance whiskers) and P2b (high-resistance whiskers) at $T = 100$ and 200 K, at different repetition times (RT) of the pulse sequence, and at the magnetic field orientations $\mathbf{H} \parallel \mathbf{b}$ and $\mathbf{H} \perp \mathbf{b}$.

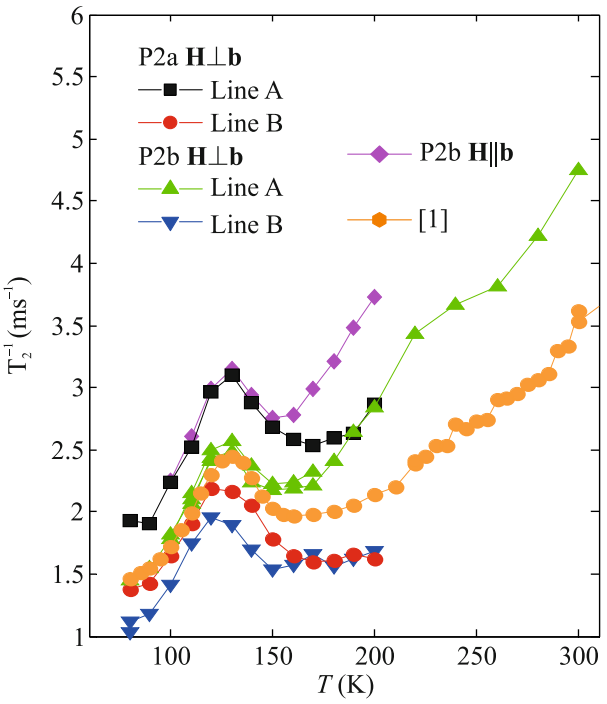


**Fig. 2.** (Color online) Temperature dependences of the relaxation rate of the transverse nuclear magnetization of $^{93}$Nb in the samples P2a and P2b at different orientations of the magnetic field **H**. The data on poorly resolved lines A and B for the sample P2b at $\mathbf{H} \parallel \mathbf{b}$ (see Fig. 1b) are averaged. Our previous data for the unoriented sample $NbS_3$-II are also presented [1].

nals of the A and B lines correspond to the most conducting chains in the sample, whereas $^{93}$Nb atoms responsible for the C line are located in nonconducting regions, which are possibly nonconducting chains.

Figures 1b and 1c show spectra of the central $^{93}$Nb NMR line in the sample P2b, where high-resistance whiskers prevail, at temperatures of 100 and 200 K in the magnetic field **H** oriented both along the axis of the whiskers $\mathbf{H} \parallel \mathbf{b}$ and across it ($\mathbf{H} \perp \mathbf{b}$), respectively. The comparison of Figs. 1a and 1b shows that the line C observed in the spectra of the sample P2a is almost absent in spectra of the sample P2b. Such qualitative difference between spectra is observed in the entire studied temperature range from 5 to 400 K. This indicates that NMR signals of the group of lines C originate from defect regions and do not belong to the $NbS_3$-II phase itself.

We note a change in the form of the spectrum under the variation of the orientation of whiskers with respect to the direction of **H** (see Figs. 1b and 1c), which reflects the quasi-one-dimensional character of the $NbS_3$ structure [15, 16].

It is clearly seen that the NMR spectra in Fig. 1 at temperatures 100 and 200 K are almost identical. This indicates that the electronic surrounding of $^{93}$Nb nuclei is not rearranged near $T_{P2} = 150$ K and, consequently, this transition is not accompanied by a change in the charge and spin states of chains.

Our study of the temperature dependence of the relaxation rate $T_2^{-1}(T)$ of the transverse nuclear magnetization provided the most significant progress in the understanding of the transition at $T_{P2}$. We measured the relaxation rate $T_2^{-1}$ on the central NMR lines in the samples P2a and P2b in the temperature range of 100–200 K separately on the lines A and B at the magnetic field orientation $\mathbf{H} \perp \mathbf{b}$ and the averaged $T_2^{-1}$ value at the orientation $\mathbf{H} \parallel \mathbf{b}$. The relaxation time of the transverse nuclear magnetization was measured at the resonant frequency using the standard two-pulse method by recording the spin echo intensity as a function of the delay time $\tau$ between the first and second radiofrequency pulses. Decay curves of the transverse magnetization component $M(\tau)$ were approximated by the function $M(0)\exp(-2\tau/T_2)$.

Figure 2 presents the temperature dependences of the measured relaxation rate $T_2^{-1}$ on the lines A and B for both samples. A maximum of $T_2^{-1}$ is observed in all temperature dependences for both groups of lines and

at two orientations of the magnetic field **H** with respect to the crystallographic **b** axis. Figure 2 also shows our previous measurements of $T_2^{-1}$ in the unoriented $NbS_3$-II sample [1]. A similarity of features on all $T_2^{-1}(T)$ curves demonstrates a high reproducibility of experimental data. As in [13], maxima in the case of $NbSe_3$ are reached at temperatures slightly below the charge density wave formation temperature. This confirms that these maxima are due to the transition at $T_{P2} = 150$ K.

We attribute the maximum of $T_2^{-1}$ with the suppression of fluctuations with decreasing temperature in the range of 150–110 K. The relaxation of the transverse nuclear magnetization is due to fluctuating fields whose correlation time is comparable with a spin-echo signal formation time of about 10–1000 μs. Thus, local maxima observed on the dependences $T_2^{-1}(T)$ in Fig. 2 correspond to the freezing of one of the sources of these fluctuating fields with decreasing temperature in the range of 110–150 K below the transition: the characteristic fluctuation times above and below the temperature of the $T_2^{-1}$ maximum are too short and too long to accelerate the transverse relaxation, respectively.

As follows from Fig. 2, the transition at $T_{P2} = 150$ K occurs not only in low-resistance samples, but also surprisingly in high-resistance ones. In this case, the maximum of $T_2^{-1}$ is observed on the $^{93}$Nb NMR lines whose frequencies correspond to *conducting* Nb *chains* in the unit cell (see Fig. 1). This means that the transition involves at least two of four pairs of Nb chains in *all* unit cells of $NbS_3$ rather than only Nb atoms near defects of the crystal [4].

Values of $T_2^{-1}$ (see Fig. 2) confirm that the compositions of the samples P2a and P2b are different: the comparison of the same lines indicates that $T_2^{-1}$ in the sample P2a is higher than that in the sample P2b. This means the prevalence of relatively low-resistance whiskers in the sample P2a.

Curves in Fig. 2 have also other features. The observed nuclear relaxation rates for the line A are higher than those for the line B, which corresponds to a higher free carrier density on A-type chains, as mentioned above. For both samples, the maximum of $T_2^{-1}(T)$ for the line B is reached at a temperature about 10 K below that for the line A, which can also be explained by longer relaxation times on B-type chains: the frequency of fluctuations becomes equal to the inverse relaxation time of this line at lower temperatures. It is also noteworthy that $T_2^{-1}$ values at the orientation $\mathbf{H} \parallel \mathbf{b}$ are higher than those at the orientation $\mathbf{H} \perp \mathbf{b}$. This can be interpreted as a small anisotropy of fluctuating fields on $^{93}$Nb nuclei: the amplitude of fluctuating fields along the **b** axis of chains is larger than that across the **b** axis.

The relaxation rate of the longitudinal nuclear magnetization of $T_1^{-1}(T)$ was also measured at different temperatures, but the corresponding temperature dependence exhibits no local maxima near the transition temperature $T_{P2} = 150$ K. The maximum longitudinal relaxation rate should be generally observed under the condition that the frequency of fluctuating fields coincides with the frequency 79 MHz of the observed NMR signal. Unlike the relaxation of the longitudinal nuclear magnetization, the relaxation of the transverse nuclear magnetization is due to slower fluctuating fields whose correlation time is about several microseconds. The absence of the maximum in the $T_1^{-1}(T)$ dependence can mean that the lattice vibrations belonging to the mode frozen at $T_{P2}$ are sufficiently slow even above $T_{P2}$, and do not affect the relaxation of the longitudinal nuclear magnetization at any temperatures. This is an important difference of the transition in $NbS_3$-II at 150 K from the transition in $NbSe_3$ at 140 K [13].

The relaxation rate $T_2^{-1}$ is almost doubled in $NbSe_3$ [13], whereas it increases only by approximately 30% in $NbS_3$-II. This can mean that the source of fluctuations is minor or remote. Furthermore, as seen in Fig. 1, the positions of $^{93}$Nb NMR spectral lines do not change in the temperature range of 100–200 K. This indicates that magnetic fields on nuclei remain unchanged. Therefore, the fluctuating field disappearing near 130 K is most probably electric.

Thus, the observation of the maximum in the temperature dependence of the relaxation rate $T_2^{-1}$ on all NMR lines means that the appearance (or critical slowing-down) of a certain ordering involving **all types** of conducting chains occurs near $T_{P2} = 150$ K in both low- and high-resistance $NbS_3$-II samples. For this reason, we more carefully analyzed the transport properties of high-resistance $NbS_3$-II samples. The $\sigma_s(T)$ dependence for such samples follows an activation law from 330 K down to at least 75 K. The maximum activation energy $\Delta \approx 2000$ K is observed in samples without signatures of the transition at $T_{P2}$ [1, 5] in agreement with photoconductivity data: $2\Delta = 430$ meV ($2 \times 2500$ K) [17]. The current–voltage characteristics of high-resistance $NbS_3$-II samples are nonlinear in the range from $T_{P1}$ down to liquid helium temperatures [6]. In entire this temperature range, nonlinearity is due to the sliding of CDW-1. This is clear, in particular, from the temperature dependence of the threshold field $E_t$: as seen in Fig. 3, the threshold field, which was identified by the beginning of nonlinearity, increases linearly with a decrease in the temperature from 300 to about 30 K. It is noteworthy that such a $E_t(T)$ dependence is not observed in other

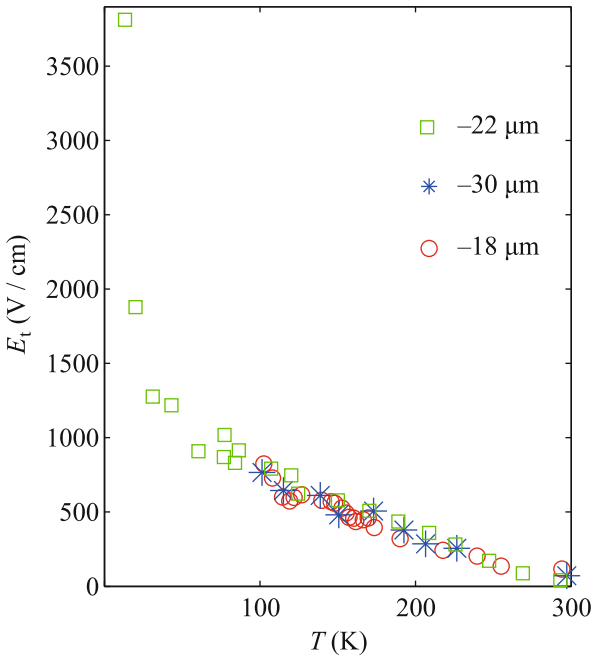


**Fig. 3.** (Color online) Temperature dependences of the threshold field $E_t$ for the high-resistance samples $NbS_3$-II no. 1 (22 μm × 0.01 μm$^2$), no. 2 (18 μm × 0.01 μm$^2$), and no. 3 (30 μm × 0.007 μm$^2$).

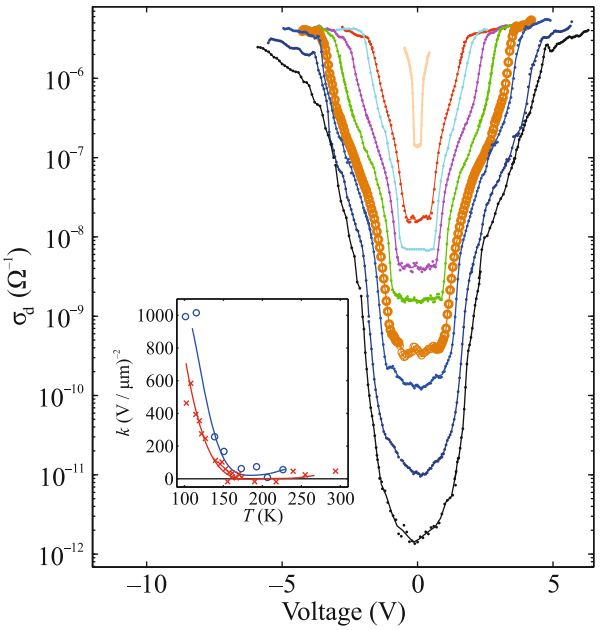


**Fig. 4.** (Color online) Differential conductivity $\sigma_d$ versus the voltage $V$ for sample no. 2 at $T$ = (from bottom to top) 101, 115, 139, 151 (marked by circles), 173, 193, 206, 226 247, and 297 K. The inset shows the temperature dependences of the parameter $k$ (see the main text) characterizing the degree of smearing of the current–voltage characteristic below $E_t$ for samples (○) no. 2 and (×) no. 3. Solid lines are drawn by eye.

quasi-one-dimensional charge density wave conductors. A nearly linear $E_t(T)$ dependence was previously observed only in rare-earth tritellurides, which are quasi-two-dimensional compounds [18, 19].

Although significant features near 150 K are not seen in $E_t(T)$ dependences (see Fig. 3), the smearing of the threshold is observed in the current–voltage characteristic below 150 K: the depinning of CDW-1 becomes less sharp. This is seen in Fig. 4, where the dependences of the differential conductivity $\sigma_d$ on the voltage $V$ are shown for one of the samples. To quantitatively describe the smearing, the $\sigma_d(E)$ curves in the field region below the threshold were approximated by a quadratic polynomial $\sigma_d(E)/\sigma_d(0) = 1 + kE^2$. The temperature dependence of the coefficient $k$ is shown in the inset of Fig. 4 for two high-resistance samples. It is seen that the increase in smearing begins just near 150 K; i.e., this temperature is also specific for the high-resistance samples.

Trying to consistently explain experimental data, we assumed that the phase transition with the formation of a superstructure occurs in all $NbS_3$-II samples at 150 K through a non-Peierls mechanism. One of the possibilities is a Jahn–Teller transition (see, e.g., [20]). The lattice distortion in high-resistance samples weakly affects transport properties. In particular, the smearing of the threshold field of CDW-1 below 150 K can be due to the reduction of the symmetry of the lattice. The wave vector of lattice distortion $\mathbf{q}_2$ in low-resistance samples is close to the doubled Fermi wave vector for electrons remaining free below $T_{P1}$. These electrons can be coupled to sulfur vacancies and be located in minibands ("pockets"), which are associated with defects of the lattice. Thus, these electrons below $T_{P2}$ are in a dielectric state and form CDW-2.

A more probable mechanism of the lattice distortion is a Keldysh–Kopaev transition [21], which is also known as the formation of an excitonic insulator [22]. It was assumed in [1] that a mechanism of the transition, which was proposed for a narrow-gap semiconductor, occurs at $T_{P2}$; $NbS_3$-II below two Peierls transitions (at $T_{P0}$ and $T_{P1}$) can be such a semiconductor. According to [23], this transition, as well as the Peierls transition, can be considered as one of the particular cases of the formation of the excitonic insulator. The transition in the narrow-gap semiconductor is possible if the band gap is smaller than the exciton binding energy. In this case, excitons are spontaneously formed and a new electronic state is developed. If the maximum and minimum of the hole and electron bands in the $k$ space are shifted, the vector connecting them determines the wave vector of a possible charge modulation, i.e., an excitonic charge density wave. If the Fermi level is near the middle of the band gap, which corresponds to the case of the stoichiometric composition of $NbS_3$, the sample is in the dielectric

state already above $T_{P2}$, and the transition is hardly observed in $\sigma_s(T)$.

Although the sliding of such charge density wave has not yet been discussed, it can be assumed that it is possible. This charge density wave in the intrinsic semiconductor is uncharged, i.e., contains the same numbers of electrons and holes. This is clear from the electron–hole symmetry of the system. The excess of electrons arises in samples with sulfur vacancies, and it has been assumed that the charge density wave becomes charged with the charge density proportional to the degree of doping by S vacancies. This mechanism explains the bulk character of CDW-2, the universality of its formation in $NbS_3$-II samples of all types, and the variation of the ratio $j_{CDW}/f$ in a wide interval [1].

We also mention the recent processing of X-ray diffraction data obtained on $NbS_3$-II crystals in synchrotron radiation. Diffraction patterns were recorded in a wide temperature range with a step of 10 K. It was found that a diffuse satellite with the components $n(4\mathbf{c}^*) + m(\mathbf{a}^* - \mathbf{c})$, where $n$ and $m$ are integers, and the component $0.5\mathbf{b}^*$ is observed at temperatures $T \geq 150$ K. The appearance of the reflection $4\mathbf{c}^*$ corresponds to a decrease in the period along the **c** axis by a factor of 4. Thus, the parameters of a fluctuation-induced structure correspond to the $NbS_3$ phase-I unit cell [2]. The possibility of a continuous transition to phase I is consistent with the model [24], according to which the unit cell of the structure of phase II can be approximately obtained by the quadruple replication of the unit cell of the basic structure of the $NbS_3$ phase I in the **c** direction. Taking into account these data, the NMR results can be interpreted as follows: the mode frozen below 150 K corresponds to the fluctuation approach of phase II to phase I. Doubling in the **b** direction above 150 K confirms this assumption. Fluctuations suppress CDW-2 above 150 K and can lead to an increase and smearing of the depinning threshold field of this charge density wave. This explanation remains the nature of CDW-2 itself open.

To conclude, the freezing (critical decrease in the frequency) of a certain minor mode equidistant from Nb atoms located at all sites of the lattice, which do not belong to defects of the crystal, occurs in $NbS_3$-II samples of all types at $T_{P2} = 150$ K. This lattice distortion explains the appearance of CDW-2 in low-resistance $NbS_3$-II samples and the smearing of the depinning threshold field of CDW-1 below $T_{P2}$ in high-resistance samples.

## ACKNOWLEDGMENTS

We are grateful to A.A. Bosak for assistance in measurements and processing of experimental data.

## FUNDING

The electrophysical studies of $NbS_3$ performed by S.G. Zybtsev was supported by the Russian Science Foundation (project no. 22-12-00319). The analysis of the data carried out by V.Ya. Pokrovskii was supported by the Ministry of Science and Higher Education of the Russian Federation (state assignment for the Kotelnikov Institute of Radioengineering and Electronics, Russian Academy of Sciences).

## CONFLICT OF INTEREST

The authors of this work declare that they have no conflicts of interest.

## OPEN ACCESS



## REFERENCES

1. S. G. Zybtsev, V. Ya. Pokrovskii, V. F. Nasretdinova, et al., Phys. Rev. B **95**, 035110 (2017).
2. P. Monceau, Adv. Phys. **61**, 325 (2012).
3. S. G. Zybtsev, V. Ya. Pokrovskii, V. F. Nasretdinova, S. V. Zaitsev-Zotov, E. Zupanic, M. van Midden, and W. Wu. Pai, J. Alloys Compd. **854**, 157098 (2021).
4. E. Zupanic, H. J. P. van Midden, M. van Midden, S. Sturm, E. Tchernychova, V. Ya. Pokrovskii, S. G. Zybtsev, V. F. Nasretdinova, S. V. Zaitsev-Zotov, W. T. Chen, W. Wu. Pai, J. C. Bennett, and A. Prodan, Phys. Rev. B **98**, 174113 (2018).
5. S. G. Zybtsev, V. Ya. Pokrovskii, V. F. Nasretdinova, S. V. Zaitsev-Zotov, V. V. Pryadun, E. S. Kozlyakova, O. S. Volkova, A. N. Vasiliev, W. W. Pai, and D. Staresinic, Phys. Rev. B **99**, 235155 (2019).
6. S. G. Zybtsev, V. Ya. Pokrovskii, V. F. Nasretdinova, and S. V. Zaitsev-Zotov, J. Commun. Technol. Electron. **63**, 1053 (2018).
7. T. Iwazumi, M. Izumi, K. Uchinokura, R. Yoshizaki, and E. Matsuura, Phys. B (Amsterdam, Neth.) **143**, 255 (1986).
8. S. G. Zybtsev, N. Yu. Tabachkova, V. Ya. Pokrovskii, S. A. Nikonov, A. A. Maizlakh, and S. V. Zaitsev-Zotov, JETP Lett. **114**, 40 (2021).
9. W. W. Pai, M. W. Chu, W. T. Chen, V. Ya. Pokrovskii, S. V. Zaitsev-Zotov, S. G. Zybtsev, V. F. Nasretdinova,

M. D. Ustenko, E. Zupanic, H. J. P. van Midden, M. van Midden, S. Sturm, A. Prodan, E. Tchernychova, and J. C. Bennett, in *Proceedings of the 22nd International Symposium on Nanophysics and Nanoelectronics* (Nizhegor. Gos. Univ. Lobachevskogo, N. Novgorod, 2018), Vol. 1, p. 285.

10. X. Xi, L. Zhao, Z. Wang, H. Berger, L. Forro, J. Shan, and K. F. Mak, Nat. Nanotechnol. **10**, 765 (2015).
11. C. Sergio, M. R. Sinko, D. P. Gopalan, N. Sivadas, K. L. Seyler, K. Watanabe, T. Taniguchi, A. W. Tsen, X. Xu, Di Xiao, and B. M. Hunt, Nat. Commun. **9**, 1 (2018).
12. E. Navarro-Moratalla, J. O. Island, S. Manas-Valero, E. Pinilla-Cienfuegos, A. Castellanos-Gomez, J. Quereda, G. Rubio-Bollinger, L. Chirolli, J. A. Silva-Guillen, N. Agrait, G. A. Steele, F. Guinea, H. S. J. van der Zant, and E. Coronado, Nat. Commun. **7**, 1 (2016).
13. B. H. Suits and C. P. Slichter, Phys. Rev. B **29**, 41 (1984).
14. W. G. Clark, M. E. Hanson, F. Lefloch, and P. Segransan, Rev. Sci. Instrum. **66**, 2453 (1995).
15. I. Mukhamedshin, in *Proceedings of the Workshop on Magnetic Resonance of Correlated Electron Materials, September 17–23, 2023, Dresden, Germany,* p. 82. https://www.ifw-dresden.de/uploads/users/155/uploads/ abstracts_fin2.pdf.
16. A. S. Semakin, I. R. Mukhamedshin, S. G. Zybtsev, and V. Ya. Pokrovskii, in *Proceedings of the 28th International Symposium on Nanophysics and Nanoelectronics, March 11–15, 2024* (Nizhegor. Gos. Univ. Lobachevskogo, N. Novgorod, 2024), V. 2, p. 789.
17. V. Nasretdinova, V. Ya. Pokrovskii, S. V. Zaitsev-Zotov, and S. G. Zybtsev, in *Nonequilibrium Phenomena in Complex Matter: New Observations and New Theories, Proceedings of the Conference, Ambrož, Krvavec, Slovenia, December 13–16, 2015* (Jožef Stefan Inst., Ljubljana, 2016), p. 46.
18. A. A. Sinchenko, P. Lejay, O. Leynaud, and P. Monceau, Phys. Rev. B **93**, 235141 (2016).
19. A. V. Frolov, A. P. Orlov, A. A. Sinchenko, and P. Monceau, JETP Lett. **109**, 203 (2019).
20. M. Holt, P. Zschack, H. Hong, M. Y. Chou, and T.-C. Chiang, Phys. Rev. Lett. **86**, 3799 (2001).
21. L. V. Keldysh and Yu. V. Kopaev, Sov. Phys. Solid State **6**, 2219 (1964).
22. W. Kohn, Phys. Rev. Lett. **19**, 439 (1967).
23. *Physical Encyclopedia,* Ed. by A. M. Prokhorov (Sov. Entsikl., Moscow, 1988) [in Russian]. https://dic.academic.ru/dic.nsf/enc_physics/5271/.
24. A. Prodan, A. Budkowski, F. W. Boswell, V. Marinkovic, J. C. Bennett, and J. M. Corbett, J. Phys. C: Solid State Phys. **21**, 4171 (1988).

*Translated by R. Tyapaev*